Electronic Supplementary Material (ESI) for Journal of Materials Chemistry A.

Supporting Information

An ultrathin and highly efficient interlayer for lithium-sulfur batteries with high sulfur loading and lean electrolyte

Xialu Fan,[ab] Yingqi Liu,[c] Junyang Tan,[c] Shan Yang,[ad] Xiaoyin Zhang,[ab] Bilu Liu,[c] Huiming Cheng,[ae] Zhenhua Sun*[ab] and Feng Li*[abf]

* Zhenhua Sun, zhsun@imr.ac.cn; Feng Li, fli@imr.ac.cn

[a] *Shenyang National Laboratory for Materials Science, Institute of Metal Research, Chinese Academy of Sciences, Shenyang, 110016, China*

[b] *School of Materials Science and Engineering, University of Science and Technology of China, Hefei, 230026, China*

[c] *Shenzhen Geim Graphene Center, Tsinghua-Berkeley Shenzhen Institute & Tsinghua Shenzhen International Graduate School, Tsinghua University, Shenzhen 518055, China*

[d] *School of Chemical Engineering, Sichuan University, Chengdu 610065, China*

[e] *Institute of Technology for Carbon Neutrality, Shenzhen Institute of Advanced Technology, Chinese Academy of Sciences, Shenzhen 518055, China*

[f] *Dalian National Laboratory for Clean Energy, Dalian 116023, China.*

Calculation of IEI (H_{mass}, Z_{mass}) in detail:

A normalized “the ratio of areal loading of interlayer to sulfur (I/S)” was proposed and “interlayer efficiency index (IEI)” was obtained by I/S to quantify the efficiency of interlayers at a certain current density. The schematic of a Li-S pouch cell with a multilayer sulfur cathode (double side coating) and lithium anode is shown in Fig. S4a. To simplify the analysis, a simple model with Cu foil, lithium anode, separator, interlayer, sulfur cathode, and Al foil is presented for calculation and discussion (Fig. S4b). In this model, all components in two Li-S pouch cells were supposed to be the same except the UHEI@PP or PP separator. Therefore, E (gravimetric energy density) can be derived by:

$$E = \frac{U \cdot Y \cdot A \cdot S}{m_{all}} \qquad (1)$$

in which U is simplified as the average voltage of Li-S cells (2.1 V), Y is the practical specific capacity based on sulfur (mAh g^{-1}), A is the areal sulfur loading with single coating (mg cm^{-2}), S is the area of sulfur cathode (cm^2), m_{all} is the total mass of all components (without the interlayer) in Li-S pouch cell (mg), E is used to represent the energy desinty (Wh kg^{-1}) of a practical cell upon discharge under specified conditions. According to the Equation (1), the gravimetric energy density of Li-S pouch cell without/with interlayer materials ($E_{\text{without/with interlayer}}$) can be deduced to:

$$E_{without\ interlayer} = \frac{U \cdot Y_{without\ interlayer} \cdot A \cdot S}{m_{all}} \qquad (2)$$

$$E_{with\ interlayer} = \frac{U \cdot Y_{with\ interlayer} \cdot A \cdot S}{m_{all} + X \cdot S} \qquad (3)$$

Here, $Y_{with\ interlayer}$ or $Y_{without\ interlayer}$ is the practical specific capacity based on sulfur (mA h g^{-1}) with or without interlayer materials at a certain current density, X is the areal mass loading of interlayer materials (mg cm^{-2}). As shown in Table S3, the normalized I/S ratio was obtained by calculating the ratio of areal loading of interlayer and sulfur. I/S was used to normalize the performance divergence with and without an interlayer at a certain current density to obtain IEI. One IEI (H_{mass}) calculated from the energy density of pouch cells was obtained as:

$$H_{mass} = \frac{E_{with\ interlayer}}{E_{without\ interlayer} \times I/S} \tag{4}$$

which means the increased ratio of gravimetric energy density by per mass (g) interlayer based on 1 g sulfur in pouch cells. However, not all interlayers reported before were tested in pouch cells. Therefore, IEI (Z_{mass}) was proposed to simplify the H_{mass}. Z_{mass} was calculated from practical specific capacity of coin cells as:

$$Z_{mass} = \frac{Y_{with\ interlayer}}{Y_{without\ interlayer} \times I/S} \tag{5}$$

which means the increased ratio of practical specific capacity promoted by per mass (g) interlayers based on 1 g sulfur in coin cells. According to Equation (4) and (5):

$$H_{mass} = Z_{mass} \times \left(1 - \frac{X \cdot S}{m_{all} + X \cdot S}\right) \tag{6}$$

can be obtained. By proposing these factors, a more objective standard to measure the interlayer efficiency in this field was provided. Meanwhile, similar deduction methods can be used to evaluate the efficiency of other non-active components in Li-S batteries.

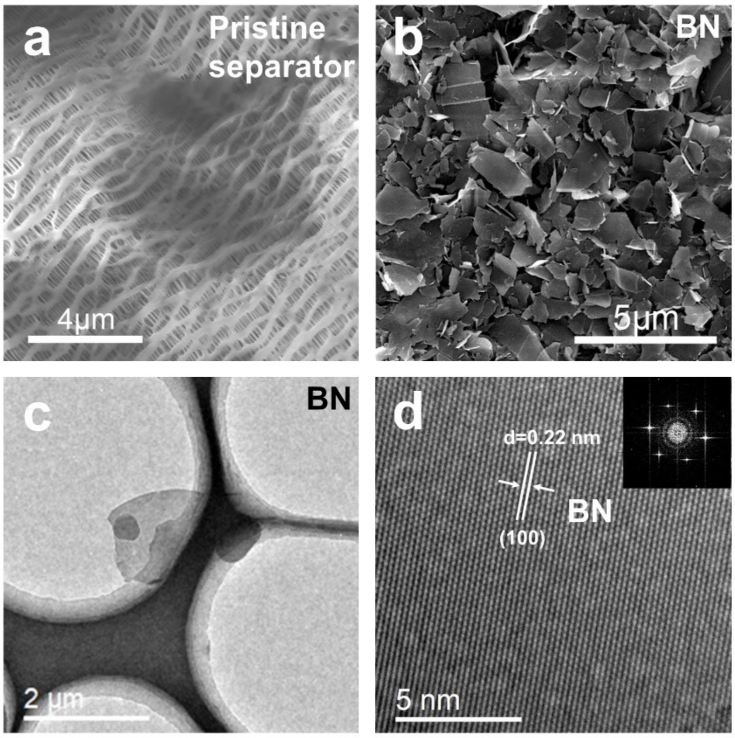

Fig. S1 SEM images of (a) pristine separator and (b) BN nanosheet. (c) TEM image of BN nanosheet. (d) HRTEM image of BN nanosheet.

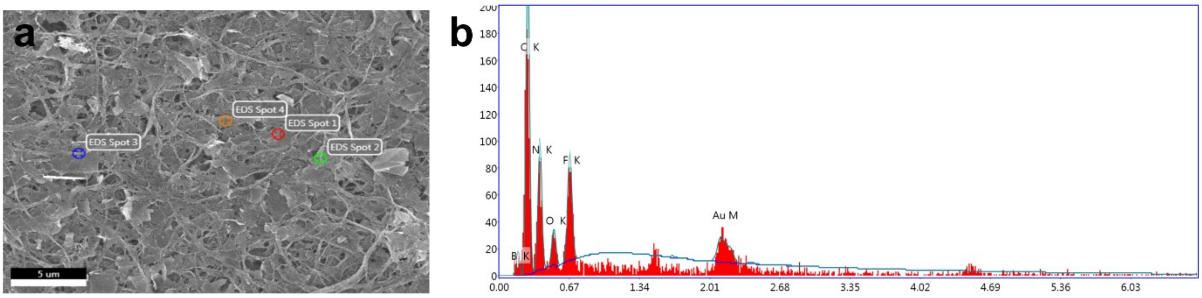

Fig. S2 (a) SEM image and (b) Corresponding EDS of UHEI.

The corresponding EDS of UHEI (Fig. S2a-b) shows the distributions of B, C, N, O, F and Au elements. The F element comes from the binder of SWCNT solution. Au comes from the metal spraying before conducting the SEM image.

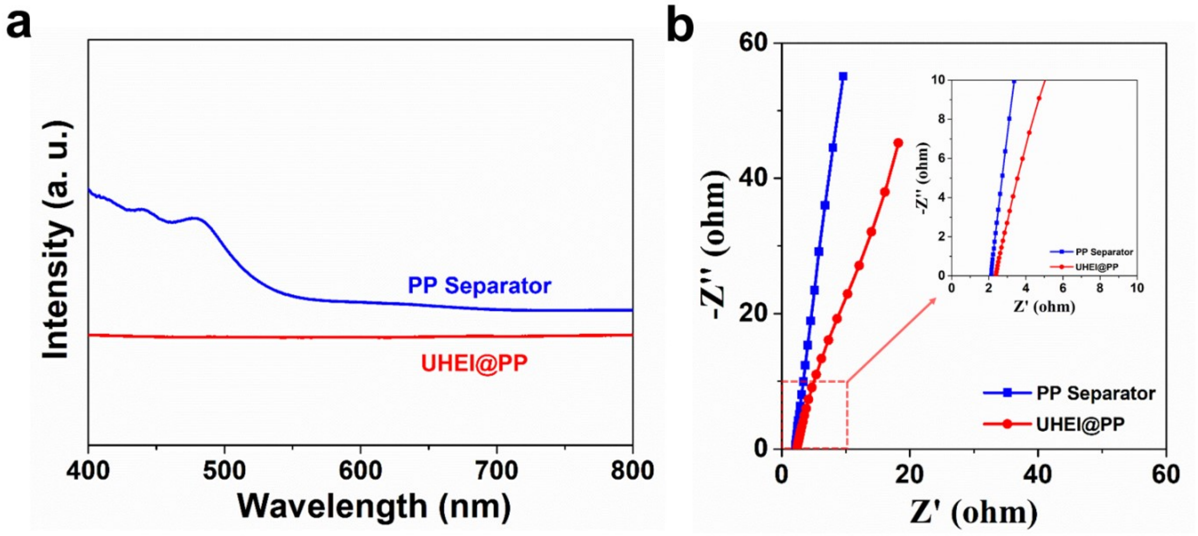

Fig. S3 (a) UV-Vis spectra of electrolyte in right chamber of H-shape device after 48 h. (b) Electrochemical impedance spectra estimating lithium conductivity.

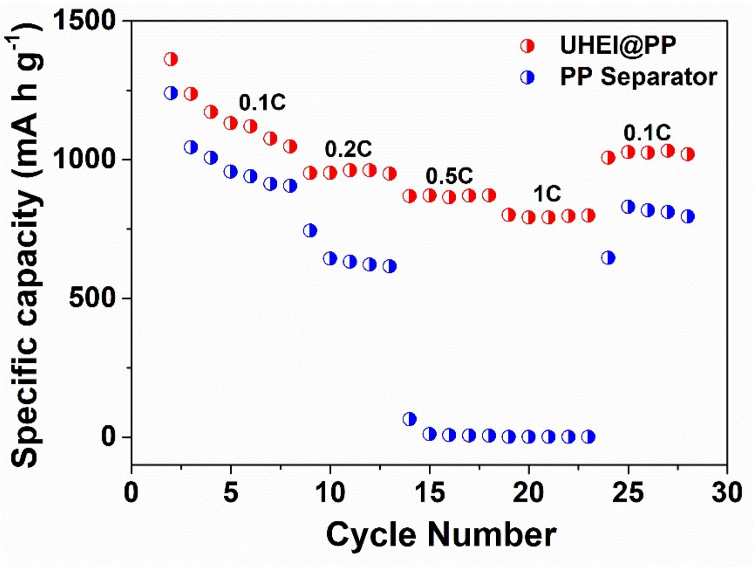

Fig. S4 Rate performances of Li-S batteries with UHEI@PP and PP separators.

The rate performance tests of Li-S coin cells with UHEI@PP and PP separators are provided in Fig. S4. When the rate was increased to 0.2, 0.5, 1 C, the capacities with UHEI@PP decreased to 961.5 mA h g^{-1}, 864.3 mA h g^{-1}, and 792.1 mA h g^{-1}, respectively and an extremely stable discharge capacity of 1025.2 mA h g^{-1} was recovered when restored to 0.1 C. On the other hand, Li-S batteries with the PP separator showed poor high-rate capability, and only 817.6 mA h g^{-1} was recovered when restored to 0.1 C. Sulfur cathodes for rate performance tests were fabricated as follows. First, CMK-3 powder (XFP03, XFNANO) and sulfur powder with a mass ratio of 4:6 were mixed in a Teflon container and heated to 155 °C for 12 h to obtain CMK-3/S. Second, the CMK-3/S, SP and polyvinylidene fluoride (PVDF) binder with a mass ratio of 7:2:1 was dispersed in N-methyl-2-pyrrolidone (NMP) to form a slurry. Finally, the slurry was coated onto a carbon-coated Al foil and dried in a vacuum oven at 60 °C for 12 h. The active material loading was kept at 1.5-2.0 mg cm^{-2}.

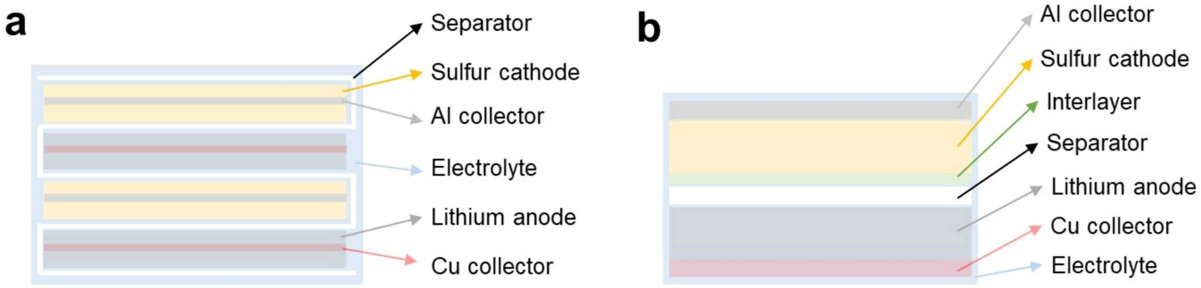

Multilayer Li-S pouch cell
(Double side coating)

Model for E calculation
(Single side coating)

Fig. S5 The schematic illustration of the cross sectional (a) Multilayer Li-S pouch cell with double side coating. (b) A simplified cell model for calculating E with single side coating.

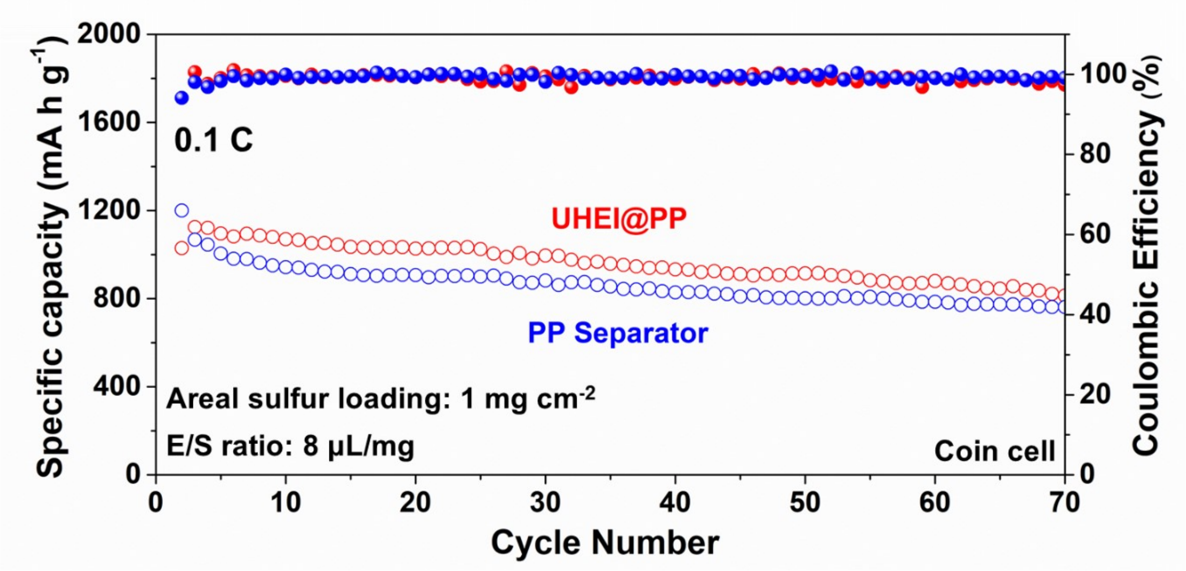

Fig. S6 Cycling stability and coulombic efficiency of Li-S coin cells with UHEI@PP and PP separator at 0.1 C under lean electrolyte conditions (E/S ratio = 8 μL mg^{-1}) for 70 cycles.

Table S1. Summary of different electrochemical parameters for Li-S batteries with UHEI@PP and PP separator.

Parameters	PP separator	UHEI@PP
Li^+ conductivity (mS cm^{-1})	0.396	0.373
Li^+ transfer number	0.66	0.69

Table S2. Comparison of the UHEI with other interlayers for Li-S batteries.

Materials	Sulfur loading (mg cm^{-2})	High plateau ratio	Low plateau ratio	Thickness
P/C-C-N-Co[1]	1	1.74	1.58	10 μm
CGF[2]	1.2	1.67	1.23	30 μm
	5.3	0.82	4.06	
NCM[3]	1.5	0.97	1.32	10 μm
	4	1.27	1.56	
ZnHMT[4]	4.5	1.33	1.31	1 nm
μFGF-MoS_2/C-TiN[5]	2.5	1.6	3.02	30 μm
ZnS/NCNS[6]	1.5	1.32	1.3	No data
TiB_2@G[7]	1.5	1.58	1.73	12.5 μm
PZI[8]	2.2	0.98	1.01	0.2 μm
	4.5	1	1.04	
	5.8	1.02	1.06	
UHEI*	2	1.32	1.53	0.86 μm
	5	1.83	2.08	
	10	16.95	2.91	

*: this work

Table S3. Comparison of the UHEI with other interlayers for Li-S batteries.

Materials	Sulfur loading (mg cm^{-2})	Interlayer loading (mg cm^{-2})	Interlayer thickness (μm)	I/S	Z_{mass} (100 cycles)
CGF[2]	1.2	0.3	30	0.25	5.52 (0.2 C)
NCM[3]	1.5	0.9	10	0.60	3.15 (0.2 C)
ZnHMT[4]	4.5	0.5	10	0.11	10.60 (0.1 C)
AS PC-Sn_4P_3[9]	1	0.15	4	0.15	9.18 (0.2 C)
HC-PDDA[10]	1.2	0.30	15	0.25	7.29 (0.2 C)
PPZ-HG-CCP[11]	1.5	3.1	50	2.07	0.62 (0.2 C)
PM (0.4 M)-CNT[12]	0.9	0.16	4	0.18	7.91 (0.2 C)
UHEI*	4.1	0.17	0.86	0.04	182.30 (0.2 C)

*: this work

References

1 Y. Li, P. Zhou, H. Li, T. Gao, L. Zhou, Y. Zhang, N. Xiao, Z. Xia, L. Wang, Q. Zhang, L. Gu and S. Guo, *Small Methods*, 2020, **4**, 1900701.

2 H. J. Peng, D. W. Wang, J. Q. Huang, X. B. Cheng, Z. Yuan, F. Wei and Q. Zhang, *Adv. Sci.*, 2016, **3**, 1500268.

3 W. L. Cai, G. R. Li, K. L. Zhang, G. N. Xiao, C. Wang, K. F. Ye, Z. W. Chen, Y. C. Zhu and Y. T. Qian, *Adv. Funct. Mater.*, 2018, **28**, 11.

4 X. Dou, G. Li, W. Zhang, F. Lu, D. Luo, W. Liu, A. Yu and Z. Chen, *J. Mater. Chem. A*, 2020, **8**, 5062-5069.

5 M. Waqas, Y. Han, D. Chen, S. Ali, C. Zhen, C. Feng, B. Yuan, J. Han and W. He, *Energy Storage Mater.*, 2020, **27**, 333-341.

6 Z. Li, F. Zhang, L. Tang, Y. Tao, H. Chen, X. Pu, Q. Xu, H. Liu, Y. Wang and Y. Xia, *Chem. Eng. J.*, 2020, **390**, 124653.

7 L. Jin, J. Ni, C. Shen, F. Peng, Q. Wu, D. Ye, J. Zheng, G. Li, C. Zhang, Z. Li and J. P. Zheng, *J. Power Sources*, 2020, **448**, 227336.

8 G. Li, F. Lu, X. Dou, X. Wang, D. Luo, H. Sun, A. Yu and Z. Chen, *J. Am. Chem. Soc.*, 2020, **142**, 3583-3592.

9 Z. Ye, Y. Jiang, T. Feng, Z. Wang, L. Li, F. Wu and R. Chen, *Nano Energy*, 2020, **70**, 104532.

10 H. Gao, S. Ning, J. Lin and X. Kang, *Energy Storage Mater.*, 2021, **40**, 312-319.

11 P. Chen, Z. Wu, T. Guo, Y. Zhou, M. Liu, X. Xia, J. Sun, L. Lu, X. Ouyang, X. Wang, Y. Fu and J. Zhu, *Adv. Mater.*, 2021, **33**, 2007549.

12 D. Xiong, S. Huang, D. Fang, D. Yan, G. Li, Y. Yan, S. Chen, Y. Liu, X. Li, Y. Von Lim, Y. Wang, B. Tian, Y. Shi and H. Y. Yang, *Small*, 2021, **17**, 2007442.